Supplementary Figures

Secreted Rhizobacterial β-Glucosidase Unlocks Coumarin-Mediated Root Iron Uptake

Xiaochen Wang[a], Xindan Xu[a,b], Xuemei Wang[a,b], Qingwen Chen[a], Qiao Zhao[d], Jinwei Wei[a], Peng Jiang[a,b], Yang Bai[a,c,c,*], and Guodong Wang[a,b,*]

[a] State Key Laboratory of Seed Innovation, Institute of Genetics and Developmental Biology, Chinese Academy of Sciences, Beijing 100101, China

[b] College of Advanced Agricultural Sciences, Chinese Academy of Sciences, Beijing 100049, China

[c] Peking-Tsinghua Center for Life Sciences, State Key Laboratory of Gene Function and Modulation Research, Peking-Tsinghua-NIBS Graduate Program, College of Life Sciences, Peking University, Beijing 100871, China.

[d] Shenzhen Key Laboratory of Synthetic Genomics, Guangdong Provincial Key Laboratory of Synthetic Genomics, Key Laboratory of Quantitative Synthetic Biology, Shenzhen Institute of Synthetic Biology, Shenzhen Institute of Advanced Technology, Chinese Academy of Sciences, Shenzhen 518055, China

* To whom correspondence should be addressed: gdwang@genetics.ac.cn and ybai@genetics.ac.cn

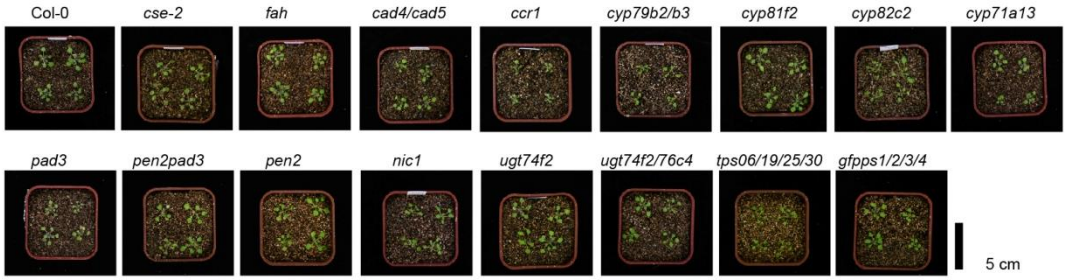

Supplementary Fig. 1. Appearance of Arabidopsis Col-0 and mutants plants grown on sterile soil.

All plants were grown under controlled short-day condition at 22^{o}C with a 10-h light/14-h dark photoperiod for 6 weeks. Scale bar = 5 cm.

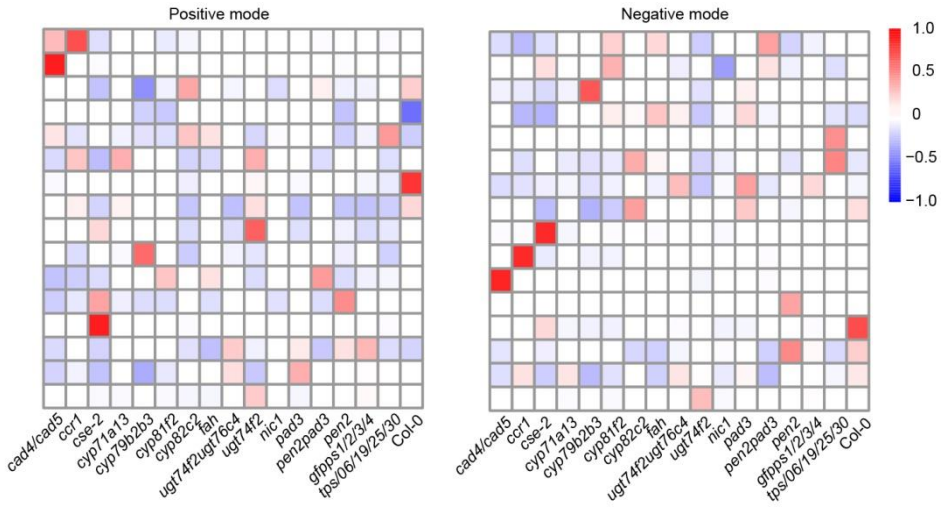

Supplementary Fig. 2. Mutants involved in biosynthesis pathways of PSMs in Arabidopsis.

Identification of genotype-specific feature modules by WGCNA network analyses. The datasets of metabolic features were collected using positive and negative ionization mode, respectively (left and right). Each module is annotated by genotype, and statistically tested by Fisher´s exact test with Yekutieli adjustment (FDR-corrected $P < 0.05$).

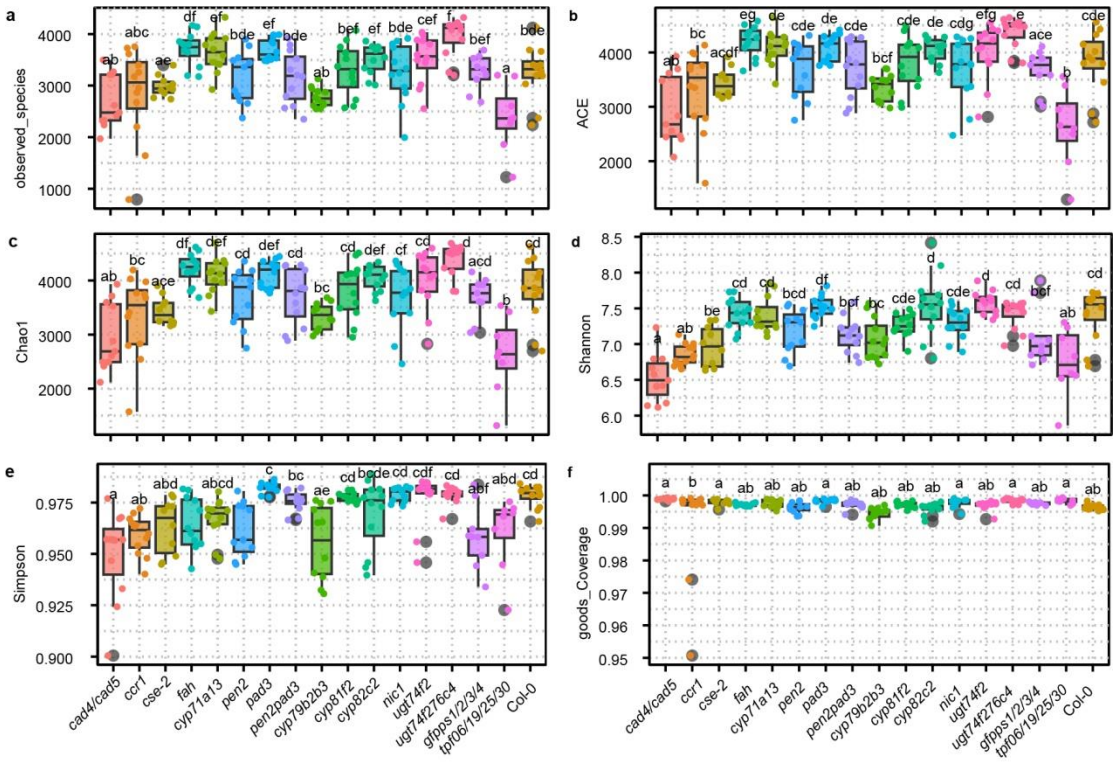

Supplementary Fig. 3. Alteration of root bacterial community of Arabidopsis plants on CAS.

Alpha diversity of root samples from CAS were analysed by ANOVA and Tukey's HSD with correction for multiple comparisons. **a,** observed species, **b,** ACE, **c,** Chao1, **d,** Shannon, **e,** Simpson, **f,** goods_couverage. **d,** Root samples of *cse-2*, *ccr1*, and *cad4cad5* have decreased diversity (Shannon index) compared to Col-0 samples. Letters indicate significant pairwise differences between groups ($P < 0.05$ by Tukey's HSD corrected for multiple comparisons.

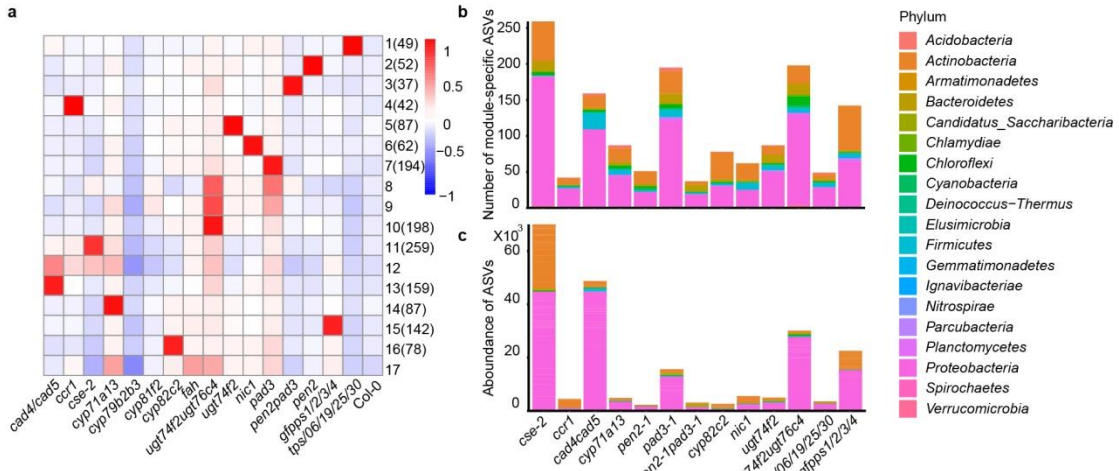

Supplementary Fig. 4. Identification of genotype-specific OTU modules by WGCNA network analyses. (A) Each module is annotated by genotype, and statistically tested by Fisher´s exact test with Yekutieli adjustment (FDR-corrected $P < 0.05$). (B) and (C) number and relative abundance of the bacterial classes specially modulized in each Arabidopsis mutant.

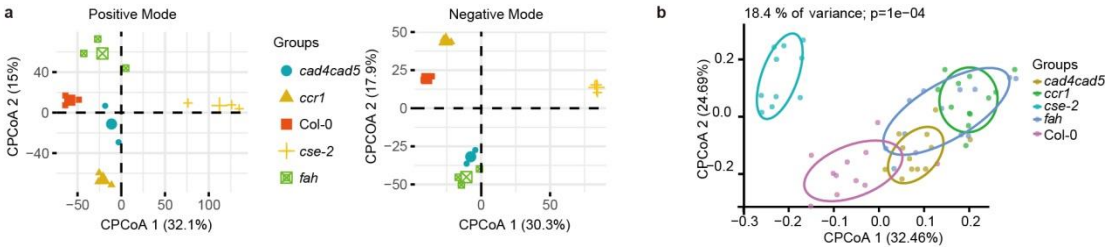

Supplementary Fig. 5. CSE is important for plant growth, rhizoshphere microbiota compostion and root metabolites compostion in CAS.

a, Constrained principal coordinate analysis (CPCoA) of Bray-Curtis dissimilarity showing lignin mutant effects on metabolome of root from Arabidopsis seedlings on CAS. **b,** Constrained ordination of root bacterial community composition of lignin pathway mutants. Ellipses delineate multivariate normal distribution at 95% confidence. *p* values represent significance of separations between genotypes determined by pairwise PERMANOVA.

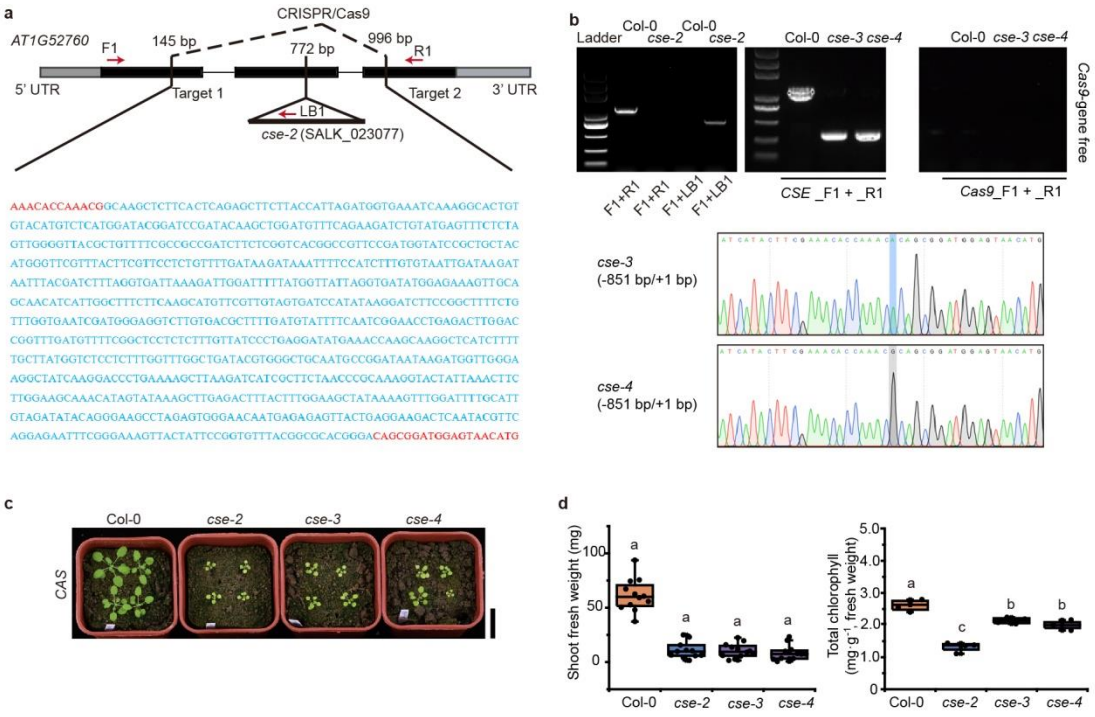

Supplementary Fig. 6. Growth deficit and chlorosis were observed on *cse* plants grown on CAS.

a, The structure of CSE gene is show with position of T-DNA insertion in cse-2 (SALK_023077) and two positions of gDNA sequences in *cse* knocked-out (KO) mutants (upper panel). Red letters indicate the original sequence. Blue letters indicate deleted sequences (lower panel).

b, Genotyping of *cse-2* mutant by PCR analysis using primers specific to genomic regions and T-DNA specifific sequence (left); Genotyping of *Cas9*-free *cse* mutants mediated by CRISPR/Cas9 using genomic specific primers (right).

c, Phenotype of Col-0 and *cse* mutants grown for 5 weeks on either Changping agricultural soil (CAS) in a short-day photoperiod (10 h light/14 h dark, 22 °C). Scale bars = 3 cm. **d,** Shoot fresh weight (SFW) and chlorophyll content in shoots of Col-0 and *cse* mutants plants grown as indicated in **c**. Bars represent means ± SD, n = 12 for SFW, n = 4 (4 seedlings per individual sample) for Chlorophyll content.

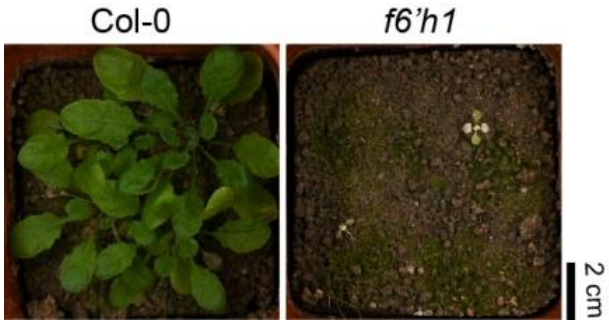

Supplementary Fig. 7. Appearance of Col-0 and *f6'h1* mutant plants on Changping agricultural soil (CAS).

Plants were grown on Changping agricultural soil (CAS) for 6-week-growth on under controlled short-day condition at 22^{o}C with a 10-h light/14-h dark photoperiod. Scale bar = 2 cm.

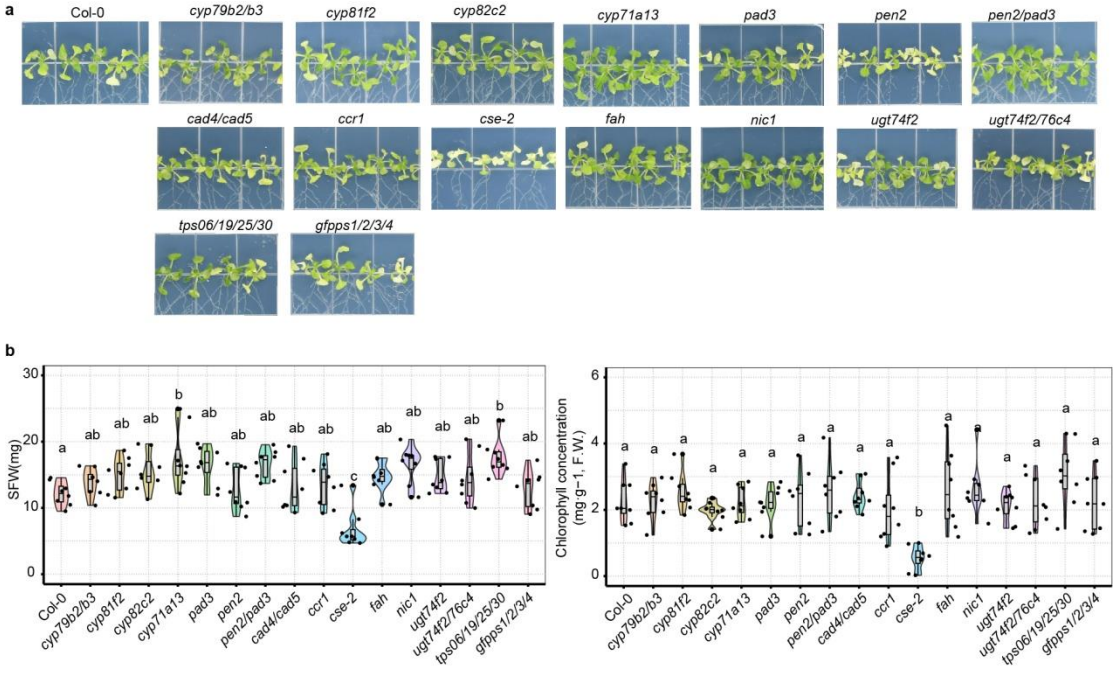

Supplementary Fig. 8. Growth deficit and chlorosis were observed on *cse* plants on the medium with Low iron availability.

a, Representative appearances of Arabidopsis plants grown for 2 weeks on medium containing low available form of iron (Low Fe) under short-day condition. Scale bar = 1 cm. **b,** Shoot fresh weight (SFW) and chlorophyll concentration of Arabidopsis seedlings grown on Low Fe medium. Data are means ± S.D. Data are from individual plant, n = 9 individual plants.

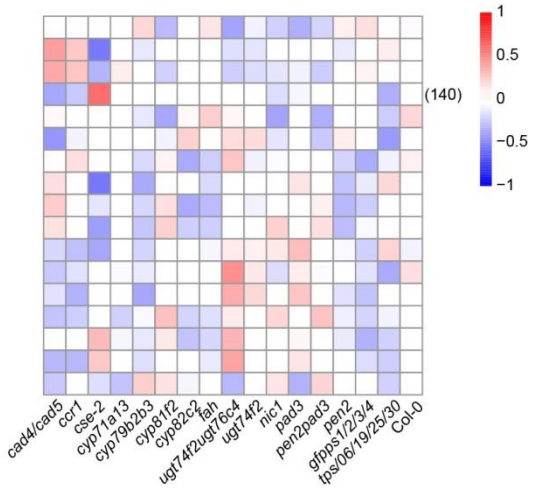

Supplementary Fig. 9. Identification of genotype-specific predicted function (FUN) modules by WGCNA network analyses. Each module is annotated by genotype, and statistically tested by Fisher´s exact test with Yekutieli adjustment (FDR-corrected $P < 0.05$).

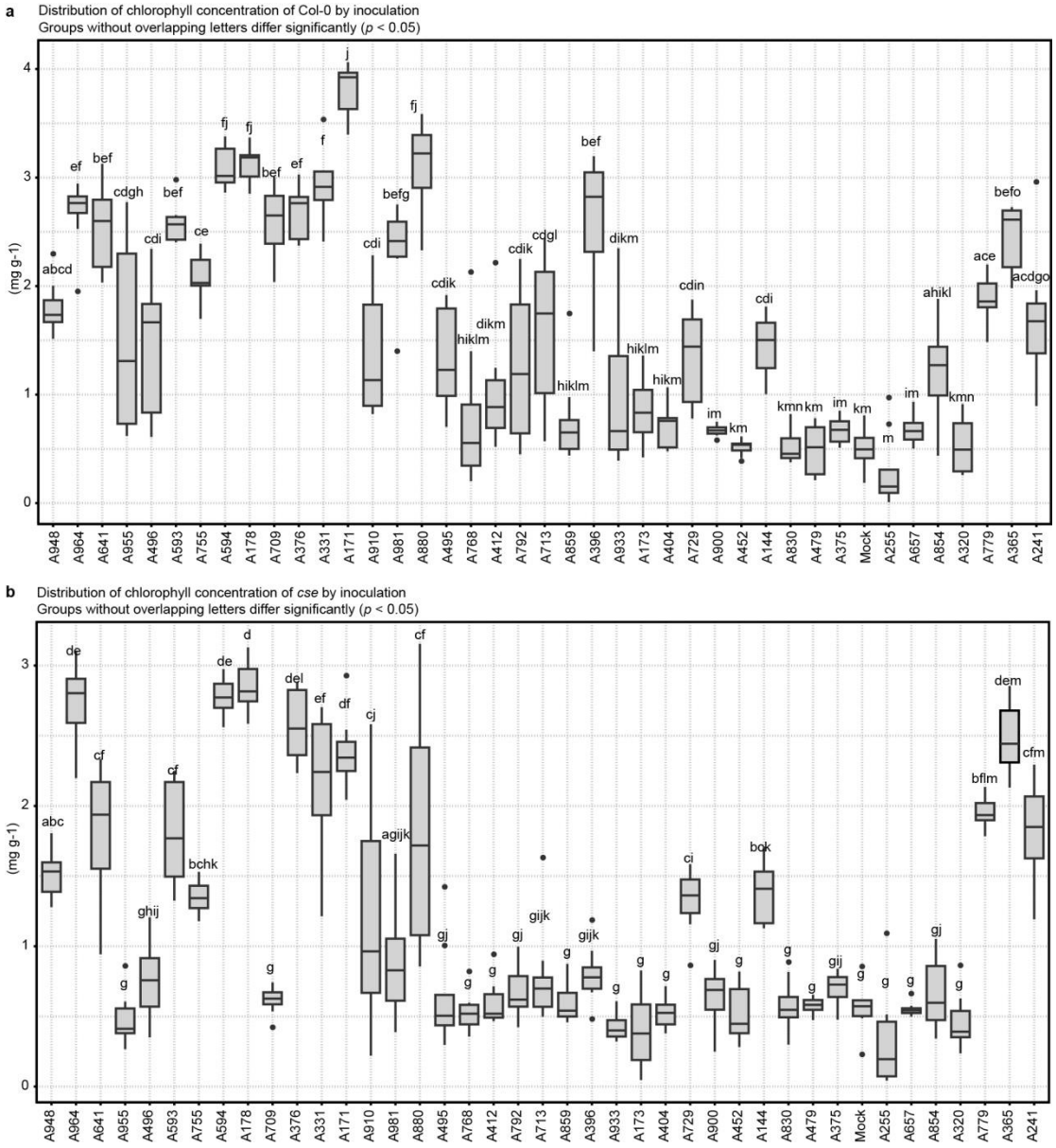

Supplementary Fig. 10. Iron-limiting growth rescue activity of SynCom strains in mono-association.

Chlorophyll concentration was measured in Col-0 **a** and *cse* **b** seedlings grown on medium with low Fe. Col-0 and *cse* plants were grown for 16 d under different Fe-limiting conditions and external pH value. Box-plots indicate means ± S.D. (n = 9 shoots) and different letters indicate significant differences ($P < 0.05$) according to one-way ANOVA with post-hoc Tukey's test at $P < 0.05$.

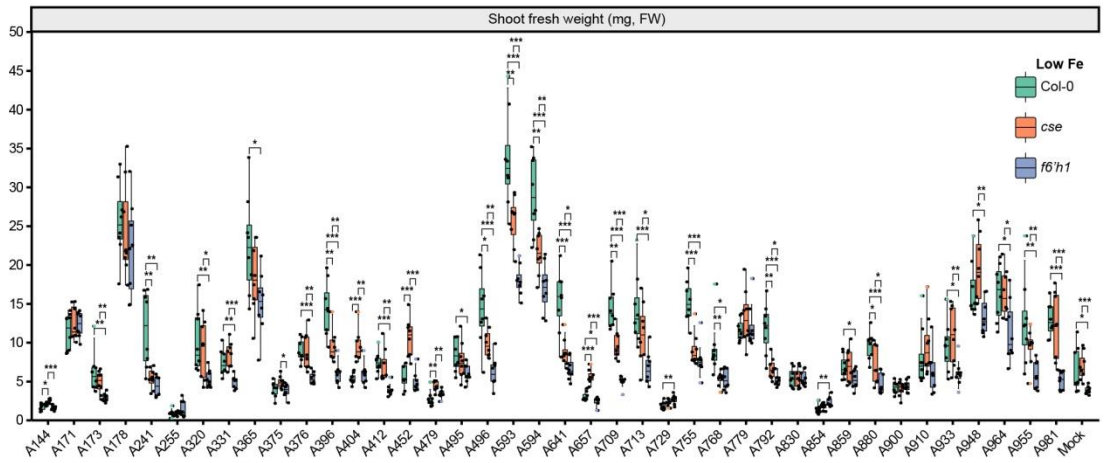

Supplementary Fig. 11. Arabidopsis-derived coumarins contribute to the rhizomicrobe mediated growth rescuing.

Shoot fresh weight and chlorophyll concentration was measured in Col-0, *cse*, and *f6'h1* seedlings grown on medium with low Fe. Col-0 and *cse* plants were grown for 16 d under different Fe-limiting conditions and external pH value. Plants were pre-cultured for 5 d on half-strength MS medium with 40 μM FeEDTA buffered with MES to pH 5.8 and then transferred to half-strength MS medium with 40 μM $FeCl_3$ buffered with MOPS to pH 7.0. Box-plots indicate means ± S.D. of 9 shoots for each treatment. **P* < 0.05, ***P* < 0.01, ****P* < 0.001 (Student's *t*-test).

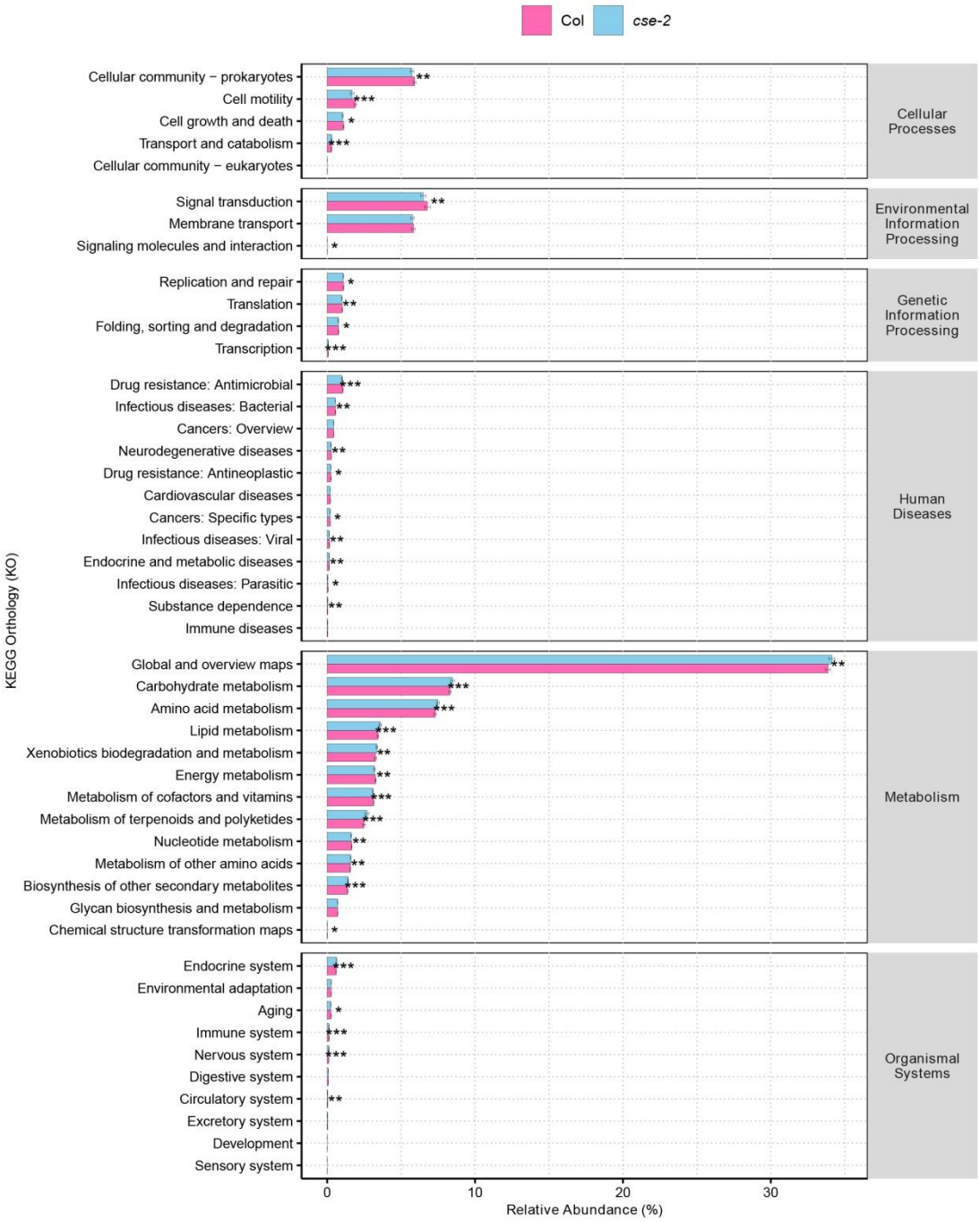

Supplementary Fig. 12. Relative abundance of the pathway categories on the Col-0 and *cse* rhizomicrobio community by Tax4Fun2 tool.

Relative abundance of the top 48 level-2 KEGG pathways for rhizosphere bacterial communities of Col-0 and *cse-2* plants. Significance level: **P* < 0.05, ***P* < 0.01, ****P* < 0.001.

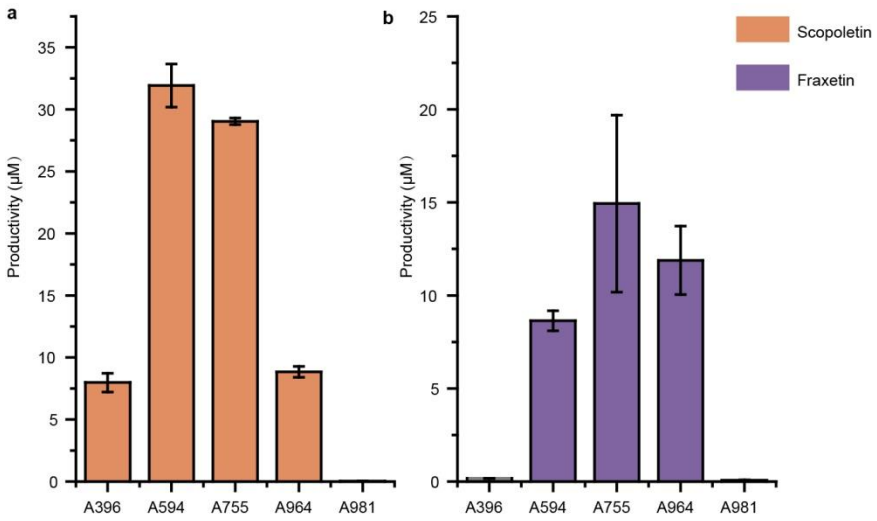

Supplementary Fig. 13. *In vivo* production of scopoletin catalyzed by rhizosphere bacteria.

Isolate strains were grown in M9 liquid medium with exogenous scopolin and fraxin supplementation for 12 h. The data represent mean ± S.D. from triplicate experiments (Supplementary Table 12).

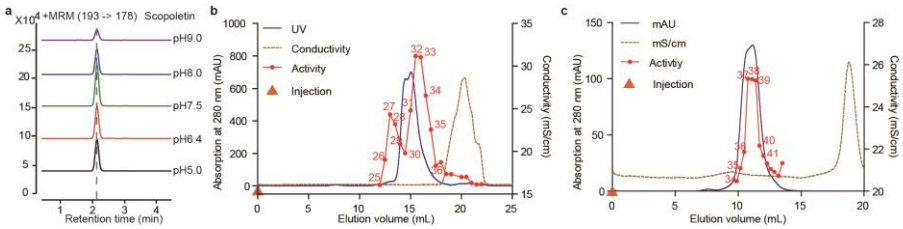

147

148 **Supplementary Fig. 14. Partial purification of hydrolase from crude**
149 **periplasmic protein extracts.**

150 **a,** Ultra-performance liquid chromatography tandem mass spectrometry
151 (UPLC-MS/MS, MRM mode) analysis of hydrolysis activity toward scopolin in
152 A594 strain's periplasmic protein extracts. The reaction conditions were
153 adjusted to series of pH values from acid to basic. **b,** Superdex 200 column
154 chromatography of hydrolysis activity in crude extracts. Fractions with
155 hydrolysis activity toward scopolin are numbered. **c,** Superdex 75 colume
156 chromatography of combined hydrolysis activity containing fractions from 31 to
157 35 from Superdex 200 chromatography. Fractions with profound hydrolysis
158 activity are numbered.

159

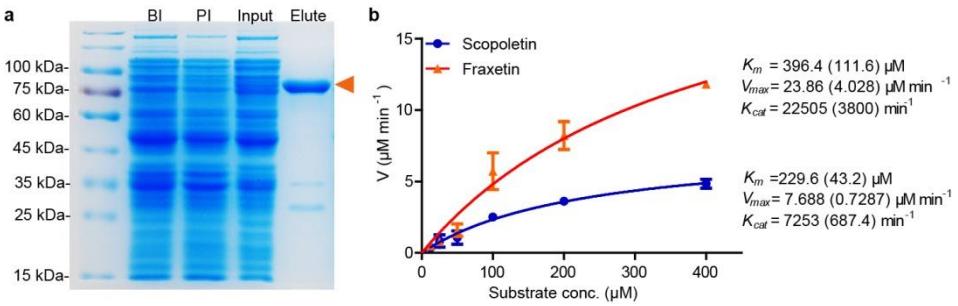

Supplementary Fig. 15. SDS-PAGE analysis of recombinant A594_07591 expressed in *E. coli*.

a, Red arrow indicates recombinant His_6-tag-A594_07591. Lane 1, total protein extracts before induction (BI) with IPTG. Lane 2, total protein extracts after induction (PI) with IPTG. Lane 3, supernatants after induction with IPTG (Input). Lane 4, purified protein after elution from Ni-NAT resin with 250 mM imidazole. **b,** Michaelis–Menten kinetics of recombinant with different concentrations of scopolin and fraxin. Error bars represent the standard error of the means (SEM) from three independent measurements of reaction velocity. The kinetic constants, *Km*, *Vmax*, and *Kcat* and their standard errors were inferred using nonlinear Michaelis-Menten curve-fitting.